Diffusion of an Anti-Transferrin Receptor Antibody in Cultured Murine Melanoma Cell Layers

Venkatramani Vijaykumar[1] and Elizabeth M. Topp[1,2]

Received June 19, 1995; accepted September 6, 1995

Purpose. The purpose of the study was to develop a cell culture system representing a layer of cells in a solid tumor, and to use the system to study factors affecting the diffusion of a binding monoclonal antibody.

Methods. A mouse melanoma cell line, B16F10, was grown on Matrigel® coated Transwell® inserts. The diffusion of a binding monoclonal antibody which recognizes the murine transferrin receptor (a-TfR) was investigated, and compared to that of an isotype-matched, nonbinding control.

Results. At a cell density of 6.4×10^5 cells/cm^2, 37°C and a donor antibody concentration of 10 nM, the permeability of the a-TfR antibody was approximately half that of the control. Blocking experiments, in which the cell layer was pretreated with excess a-TfR, resulted in equal permeabilities for a-TfR and control antibodies, suggesting that the difference in permeabilities observed in the absence of blocking is due to a-TfR binding. Experiments at 4°C and in the presence of metabolic inhibitors also equalized the permeation rates of the two antibodies, indicating that internalization of the antibody/antigen complex is important in retarding the permeation of the binding antibody.

Conclusions. In this system, the diffusion of the a-TfR antibody is retarded by binding and internalization processes. The results have implications for the use of immunoconjugates in cancer chemotherapy, and for the delivery of other binding macromolecules to tissue sites of action.

KEY WORDS: monoclonal antibody; diffusion; transferrin receptor; tumor permeation; B16F10 melanoma.

INTRODUCTION

The ideal chemotherapeutic agent selectively kills malignant cells without affecting normal cells. In recent years, monoclonal antibodies linked to cytotoxins or radioisotopes, called "immunoconjugates," have been developed as an approximation to this ideal. The antibody recognizes specific antigenic markers on the surface of malignant cells, while subsequent interaction of the cytotoxin or radioisotope with the cell causes cell death. Since binding to normal cells is minimized, the effects are targeted specifically to malignant cells, in theory improving the effectiveness of a given dose and reducing side effects.

While immunoconjugates have often been highly effective in in vitro testing, the results of human clinical trials have fallen short of ideal (1,2). Complete remissions or "cures" are rare, and the conjugates are often completely ineffective in more than half the patients tested (2). Several explanations for this low clinical efficacy have been proposed, including modulation of the tumor antigens during therapy (3), lack of specificity of an immunoconjugate for the antigens expressed in a particular patient (3) or tumor cell (4), the advanced disease state of patients in clinical trials, limitations in dose due to the patient's immune response to foreign proteins (1,2) and the rapid clearance of immunoconjugates from the bloodstream (4). An additional explanation, and one that is receiving increased attention, is that the target cells are simply inaccessible to the immunoconjugate.

A chemotherapeutic agent reaches its target cells in a number of steps. Once in the bloodstream, it must first cross the endothelial cells and underlying basement membrane of the capillaries in the tumor. Next, it must penetrate through layers of tumor cells, so that its cytotoxic activity can be displayed throughout the tumor mass. Finally, it must cause biochemical events in individual cells that lead to cell death. If any one of these steps is too slow, all of the target cells will not be destroyed, and therapeutic efficacy will be compromised. Since the capillary endothelium and basement membrane in tumors are often quite leaky, transport through the tumor tissue itself may pose the critical barrier to immunoconjugate delivery.

The penetration of an antibody through a solid tumor is, in part, a problem in mass transfer. The importance of mass transfer issues in tumor penetration has been recognized, and a number of excellent reviews on the subject have been published (5–8), most notably by R. K. Jain. Briefly, mass transfer in any physical system may be driven either by a concentration gradient or by a pressure gradient, or by both simultaneously. The former mechanism is "diffusion," while the latter is "convection." Both convection and diffusion are thought to be important in the penetration of immunoconjugates through tumors (5–8). Higher concentrations of the conjugate in the vasculature than in the tumor are expected to promote diffusion into the tumor space. At the same time, convective forces may tend to oppose penetration, since the hydrostatic pressure within some tumors has been found to be greater than that in the peripheral vasculature (5,6,8). In addition, immunoconjugate transport is expected to be slowed due to two intrinsic properties of the molecules themselves: 1) their high molecular weight (150,000 daltons or more) and 2) their high binding affinity for the cells. The expected slowing of antibody penetration by binding to tumor cell antigens has been expressed as the "binding site barrier" hypothesis (9,10).

Previous experimental and theoretical work has been directed toward understanding antibody penetration in tumors. Both animal models (10–12) and in vitro systems (13–16) have been used to study antibody penetration in tumors, and mathematical models have been proposed to describe the influences of diffusion, convection and binding on penetration kinetics (9,17,18). Despite these efforts, the factors determining the tumor penetration rate have not been clearly established. Tumors are highly heterogeneous, and may vary in cell density, in the number of target antigens per cell and in the composition of the extracellular space. The antibody portion of an immunoconjugate may be designed with varying affinity for the target antigen and, through the use of

[1] Department of Pharmaceutical Chemistry, The University of Kansas, Lawrence, Kansas 66045-2504.

[2] To whom correspondence should be addressed.

0724-8741/95/1200-1907$07.50/0

antibody fragments, with varying molecular weight. The interactions among these tissue and antibody parameters will determine the achievable penetration rates. At present, the means by which this occurs are poorly understood.

In this work, we present a cell culture system intended to represent a layer of cells in a solid tumor. Murine melanoma cells, B16F10, are cultured on treated polyester (Transwell®) filters in a planar geometry. The diffusion of an antibody to the murine transferrin receptor in these cell layers is investigated, and compared to that of an isotype matched, non-binding control. Transferrin receptor is overexpressed in many types of malignant cells due to their high iron requirements, and so has often been selected as a target antigen for immunoconjugates (19). The studies reported here demonstrate that antibody binding retards diffusive transport, in keeping with the "binding site barrier" hypothesis. Furthermore, the results suggest that internalization of the antibody/receptor complex contributes to the slowing of antibody transport in this system.

MATERIALS AND METHODS

Materials

The monoclonal antibody against the murine transferrin receptor (a-TfR, clone R17217, rat IgG_{2a}) was purchased as fluorescein isothiocyanate (FITC) and R-phycoerythrin (R-PE) labeled conjugates from Sigma Chemical Company (St. Louis, Missouri). An isotype matched control antibody that is specific for 2,4-dinitrophenol (a-DNP, clone LO-DNP-16, rat IgG_{2a}), also available as an FITC-labeled conjugate, was purchased from Zymed, Inc. (South San Francisco, California). Both were dialyzed against phosphate buffered saline overnight and stored at −20°C in small aliquots, except during an experiment when they were stored at 4°C for not more than two days. Dulbecco's modified Eagle's medium (DME), non-essential amino acids, sodium pyruvate and penicillin-streptomycin solution were purchased from JRH Biosciences (Lenexa, Kansas). Heat inactivated fetal bovine serum (FBS) was purchased from Intergen (Newark, New Jersey). Trypsin, Hank's balanced salt solution (HBSS), D-(+)-glucose, N-2-hydroxy piperazine-N″-2-ethanesulfonic acid (HEPES), phenol red free DME and sodium bicarbonate were purchased from Sigma Chemical Co., (St. Louis, Missouri). All additional buffer components were purchased from Fisher Scientific (Fairlawn, New Jersey) and were of reagent grade.

Cell Culture

The murine melanoma cell line, B16F10, was provided by Dr. I. J. Fidler, (M. D., Anderson Cancer Center, Houston, Texas) at passage 11. B16F10 is a metastatic variant of the parent murine melanoma cell line (B16F1), selected for its ability to colonize the lung. The cells were kept frozen in liquid nitrogen until use; all experiments were performed on cells between passage 14 and 25. The cells were cultured in an incubator maintained at 37°C, with 95% humidity and a 5.5% CO_2/94.5% air atmosphere. For routine culture, the cells were grown in 60 mm Petri dishes in a "growth medium" consisting of DME supplemented with 2.2 g/L sodium bicarbonate, 1% non-essential amino acids, 1 mM sodium pyruvate, 100 U/ml penicillin, 100 U/ml streptomycin and 10% FBS. Every three days, the cells were passaged by splitting 1:20 using a 0.01% trypsin/0.1% EDTA solution.

For transport experiments, the cells were grown on Transwell® inserts (cat. no. 3450, 0.4 μm pore size, 24.5 mm diameter, Corning-Costar, Cambridge, Massachusetts). The inserts were coated by adding 0.4 ml of a 1 mg/ml solution of Matrigel® (Collaborative Biomedical Products, Inc., Bedford, Massachusetts) to the surface of the Transwell® filters. Matrigel® is a reconstituted basement membrane consisting of collagen and extracellular matrix proteins, and was used in these experiments to improve the adherence of the cells to the filters, particularly at high cell densities. The Matrigel® solution was gently spread to cover the filters, and residual solution was removed by aspiration. The solution was then allowed to dry during a one hour incubation at 37°C.

In most experiments, cells were seeded onto the coated inserts at a density of 2.0×10^5 cells per well. The cells were then cultured in the growth medium described above for two days. Following this period, the growth medium was replaced with serum-free medium, having the same composition as the growth medium, but without FBS. Cells were cultured in this medium for an additional twenty-four hours prior to transport studies. Culture in serum-limited medium has been shown to enhance transferrin receptor expression in these cells (20). Under these conditions, the cell density at the time of the experiment was approximately 3×10^6 cells per well, as measured using a Coulter counter. In experiments to determine the effect of cell density on permeation, this procedure was modified. Cells were seeded at 0.5×10^5 or 2.2×10^5 cells per well, then cultured for one day in serum supplemented medium prior to the twenty-four hour incubation in serum-free medium. The resulting cell densities at the time of the transport experiments were 0.7×10^6 and 1.4×10^6 cells per well.

For control experiments designed to determine background resistance, cell-free filters were used. These were prepared by pre-coating the Transwell® filters with Matrigel®, culturing the cells in a manner identical to that used in the other experiments, detaching the cells using a 0.25% trypsin solution and then washing away the cells prior to the transport experiment. Since B16F10 cells are invasive, this procedure will result in some degradation of basement membrane components. In this way, the Matrigel® coating in control experiments was present (or degraded) to the same extent as in cell laden cultures, providing the closest control.

An identical cell culture protocol was followed for the binding studies, except that the cells were grown on Matrigel®-coated twelve-well plates (Corning-Costar, Cambridge, Massachusetts) rather than on Transwell® inserts. As with the transport studies, the cells were cultured for twenty-four hours in serum-free medium prior to binding experiments.

Electron Microscopy

Cells cultured on Transwell® inserts were examined by scanning and transmission electron microscopy. In preparation for scanning electron microscopy (SEM), cells were fixed for one hour at room temperature in 2.5% (v/v) glutaraldehyde in Hank's Balanced Salt Solution (HBSS) at pH 7.4, then postfixed for 1.5 hours on ice in HBSS with 1%

OsO_4, followed by four hours at room temperature in 0.5% uranyl acetate. After dehydration through a graded series of ethanol solutions and critical point drying using CO_2, the cell-laden membrane was mounted on a stub, sputter coated in Hummer II with Au-Pd to a thickness of 300 Å. The sample was then examined with a Hitachi 570 scanning electron microscope operated at 10 kV.

Cells were fixed, postfixed and dehydrated for transmission electron microscopy (TEM) using a procedure similar to that for SEM. Following ethanol dehydration, cells for TEM were treated with mixtures of acetone and EM-BED-812 and embedded. The preparation was then cut into 800 Å thick sections and stained for ten minutes with aqueous 2% uranyl acetate and lead citrate. The sections were examined with a JEOL 1200EXII electron microscope operated at 80 kV.

Diffusive Transport Studies

All diffusion studies were conducted in a 37°C incubator (Hotpack®, Herolein Scientific, Philadelphia, Pennsylvania) or in a 4°C cold room. While neither the oven nor the cold room provided for controlled humidity or gas phase composition, both permitted the use of an orbital shaker to provide gentle agitation of the diffusion cells. During the transport studies, the growth medium used for routine cell culture was replaced with a "transport medium." The transport medium was identical to the growth medium, except that it contained phenol red free DME to minimize interference in measurements of fluorescence intensity, 0.1% bovine serum albumin (BSA) as a blocking agent to minimize non-specific binding of the antibodies, and 20 mM HEPES as buffer. FBS was omitted from this medium to prevent possible interference from bovine transferrin. Prior to a transport experiment, the cell layers on the Transwell® inserts were washed once with warm transport medium. The inserts were then returned to the culture plates, and transport medium was added to the donor (1.45 ml) and receiver (2.6 ml) sides. The cells were then incubated for one hour to allow blocking of non-specific binding sites.

Following this incubation, a diffusion experiment was initiated by adding 50 μL of a solution of FITC-labeled antibody to the donor side of the diffusion cell. The culture plate was then agitated for five minutes at approximately 80 rpm on an orbital shaker to ensure adequate mixing. The agitation rate was then reduced to 55 rpm for the remainder of the experiment. The total duration of the experiment was four to six hours. To determine the amount of antibody transported, 100 μL aliquots were withdrawn from the receiver compartment at various times, and the fluid withdrawn was replaced with fresh transport medium. The samples were stored at 4°C for not more than five hours, and then the antibody concentration was determined as described below. At the end of the experiment, both the donor and the receiver compartment were sampled. A separate final sample from the receiver side was filtered through a 10 kD molecular weight cut-off filter (Microcon-10, Amicon, Denvers, Massachusetts). The fluorescence intensity of this filtrate was determined as a measure of antibody degradation and/or loss of fluorescent label. We found this method to be as reliable as trichloroacetic acid precipitation in measuring protein degradation. The amount of antibody retained by the cells was determined by removing the filter from the Transwell® with a scalpel, placing it in a six-well plate, and then solubilizing the cells. The cells were solubilized by the addition of 1 mL of 0.3 N KOH, incubation for one hour at 37°C and vigorous pipetting of the viscous solution. The fluorescence intensity of the solution was read directly as a measure of the antibody retention by the cells.

In some experiments, the procedures described above were modified to probe mechanisms of transport. In "blocking" experiments, cells were incubated with a ten-fold excess (100 nM) of the R-PE labeled a-TfR antibody for two hours prior to and during the transport study. The fluorescence of R-PE does not interfere with that of FITC and therefore served as a "cold" ligand to block receptor sites; an unlabeled form of this antibody is not available commercially. In experiments designed to study the effects of antibody internalization, the metabolic inhibitors sodium azide (25 mM) and 2-deoxy-D-glucose (50 mM) were added to the transport buffer during the diffusion experiment and the preceding one-hour incubation.

In each transport study, the apparent permeability was calculated from the slope of the line obtained by fitting the data to the following steady-state equation:

$$C_r = (P\ A\ C_o\ t)/V_r \quad (1)$$

where C_r is the receiver compartment concentration at any time t, P is the apparent permeability, A is the cross-sectional area available for diffusion (here, 4.7 cm^2), C_o is the initial donor compartment concentration and V_r is the receiver compartment volume. This equation is a simplification of more general equations for diffusion in plane sheets (21), and is expected to be valid when the amounts transported are small and boundary layer resistances are negligible. In these studies, the amount transported was less than 5% of the initial donor compartment concentration in all cases, and the diffusion cells were agitated to minimize boundary layer effects.

Binding Studies

The binding of the a-TfR and a-DNP antibodies to B16F10 cells was assessed in both kinetic and equilibrium studies. The kinetic experiments were performed in order to determine the time required to reach binding equilibrium. In these studies, cells were incubated in twelve-well plates at 37°C in 1.2 ml of transport medium with 5 nM of antibody. At appropriate times, the medium was removed, and the monolayers were washed three times in HBSS and then solubilized as described above. The concentration of bound antibody in this solution was determined as described in "Analytical Methods," below.

Equilibrium binding studies were conducted for the a-TfR antibody at several antibody concentrations in order to determine the binding affinity (K_a) and number of antigenic sites per cell (n). The cells were incubated at 37°C or 4°C for two hours in transport medium containing 0 to 50 nM of the antibody. Cells were then solubilized and the concentration of bound antibody determined as in the kinetic experiments. The concentration of unbound (free) antibody was determined by difference from the known amounts of total and bound antibody. The equilibrium binding constant

and maximal antibody binding per cell were obtained from a Scatchard analysis of the binding data at 4°C.

Analytical Methods

The protein concentration in stock solutions of the antibodies was determined prior to use. Antibodies were not stored as purchased, but were subjected to dialysis to remove sodium azide and any free label. As some loss and dilution is possible during dialysis, stock antibody concentrations were determined using the following formula (22):

$$C = (A_{495}/(\epsilon \times b)) * (MW \div (F/P)) \quad (2)$$

where A_{495} is the absorbance at 495 nm, ϵ is the molar absorptivity ($7 \times 10^5\ M^{-1}\ cm^{-1}$), b is the path length (1 cm), MW is the molecular weight of the protein (1.5×10^5 g/mol) and F/P is the average number of FITC molecules conjugated to each molecule of protein. The (F/P) value was 4.3 for the a-TfR antibody, and 5.1 for the a-DNP antibody, according to the manufacturers' product specifications.

Antibody concentrations in samples from the binding and transport studies were determined by measuring fluorescence intensity using a Shimadzu spectrofluorometer, model RF 5000, and comparing the values to a calibration curve prepared using the stock solution. In the transport studies, the total fluorescence intensity at each time point was corrected by subtracting the contribution of low molecular weight material to the total fluorescence intensity (see Diffusive Transport Studies). The contribution of low molecular weight material at each time was estimated from the fluorescence intensity of the filtrate measured at the end of the experiment, assuming the percentage contribution of low molecular weight material to total fluorescence was the same throughout the experiment.

The amount of antibody bound to cells in both transport and binding experiments was quantified as follows. The cells were cultured in a manner similar to that used in the binding or transport experiments, then solubilized in 0.9 ml of 0.3 N KOH. To construct a calibration curve, known concentrations of labeled antibody in 0.1 ml were added to this solution, and the fluorescence intensity measured. Standard curves constructed in this way were linear over a range of antibody concentrations of 0.1 to 1 nM at a cell density of 0.64×10^6 cells/cm^2. It is assumed in this assay that alkali solubilization destroys or precludes antigen-antibody interaction, producing a uniform mixture of solubilized cells and fluorescent protein.

RESULTS

Figure 1 shows a typical growth curve for B16F10 cells. The cells were grown on uncoated Transwell® inserts, at an initial seeding density of 1.25×10^4 cells/well. The growth curve displays a lag phase (0–2 days), followed by a period of exponential growth (2–6 days), and finally a plateau (>6 days) in which the number of cells no longer increases with time. This pattern is typical of cells in monolayer culture. The approximate doubling time for B16F10 under these conditions is sixteen hours during the exponential growth phase. This value was used to estimate cell densities for transport experiments. B16F10 cells do not display contact inhibition,

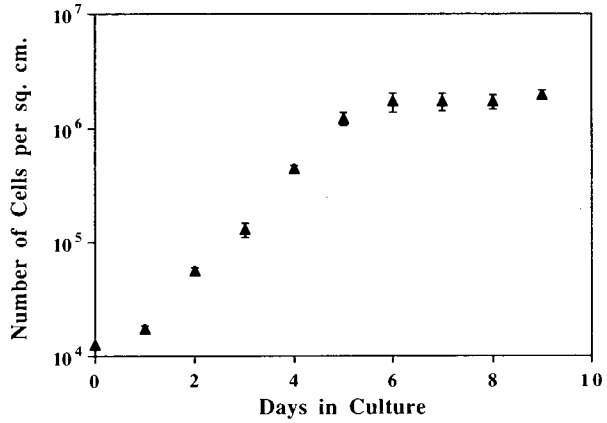

Fig. 1. Growth of B16F10 cells on Matrigel coated Transwell inserts, at a seeding density of 1.25×10^4 cells/well. n = 3.

and so form multiple layers in high density culture (see Fig. 2). Although not obvious in Figure 1 due to the semi-log scale, the standard deviation in cell number increases greatly during the plateau phase of growth. This may reflect poor cell adhesion at high cell density. In preliminary studies, it was difficult to maintain a culture at greater than 7×10^5 cells/cm^2 as the cells tended to detach from the filter during washing and handling procedures. Precoating with a 1 mg/ml solution of Matrigel® significantly improved adhesion without affecting the growth rate, and provided a more rugged culture as required for transport experiments. Higher Matrigel® concentrations altered cell shape and/or hindered cell growth. Most transport experiments were performed at a cell density of 6×10^5 cells/cm^2 (3×10^6 cells/well), which corresponds to a culture two to three cells in thickness (see Fig. 2). This density was chosen in order to obtain the maximum resistance to diffusional transport in a mechanically stable culture.

Figure 2 shows scanning (SEM) and transmission (TEM) electron micrographs of this cell culture system. Under SEM (Figure 2a), the cells exhibit the polygonal morphology characteristic of melanoma cells in culture. That multiple cell layers are formed is also evident, with cellular morphology dependent on distance from the filter. Cells that are closer to the filter support appear to have a more dendritic morphology, perhaps as a result of their attachment to the filter. In contrast, the uppermost cells appear spherical, suggesting a lack of spreading atop another cell surface. Multiple cell layers are also evident in TEM (Figure 2b). It is important to note that melanoma cells are of a neuroectodermal origin and therefore do not grow as organized sheets with the highly obstructive tight junctions characteristic of epithelial cells. Figure 2b shows that, while there are some intercellular contacts, particularly between cells near the filter support, the upper cell layers are generally discontinuous.

Figure 3 shows the kinetics of binding of the specific (a-TfR) and non-specific (a-DNP) antibodies to B16F10 cells cultured in twelve-well plates at an initial antibody concentration of 5 nM. Binding of the a-DNP antibody is complete in approximately 30 minutes, at a level of approximately 0.1×10^5 antibody molecules per cell. In contrast, binding of the a-TfR antibody occurs over approximately 2 hours, plateau-

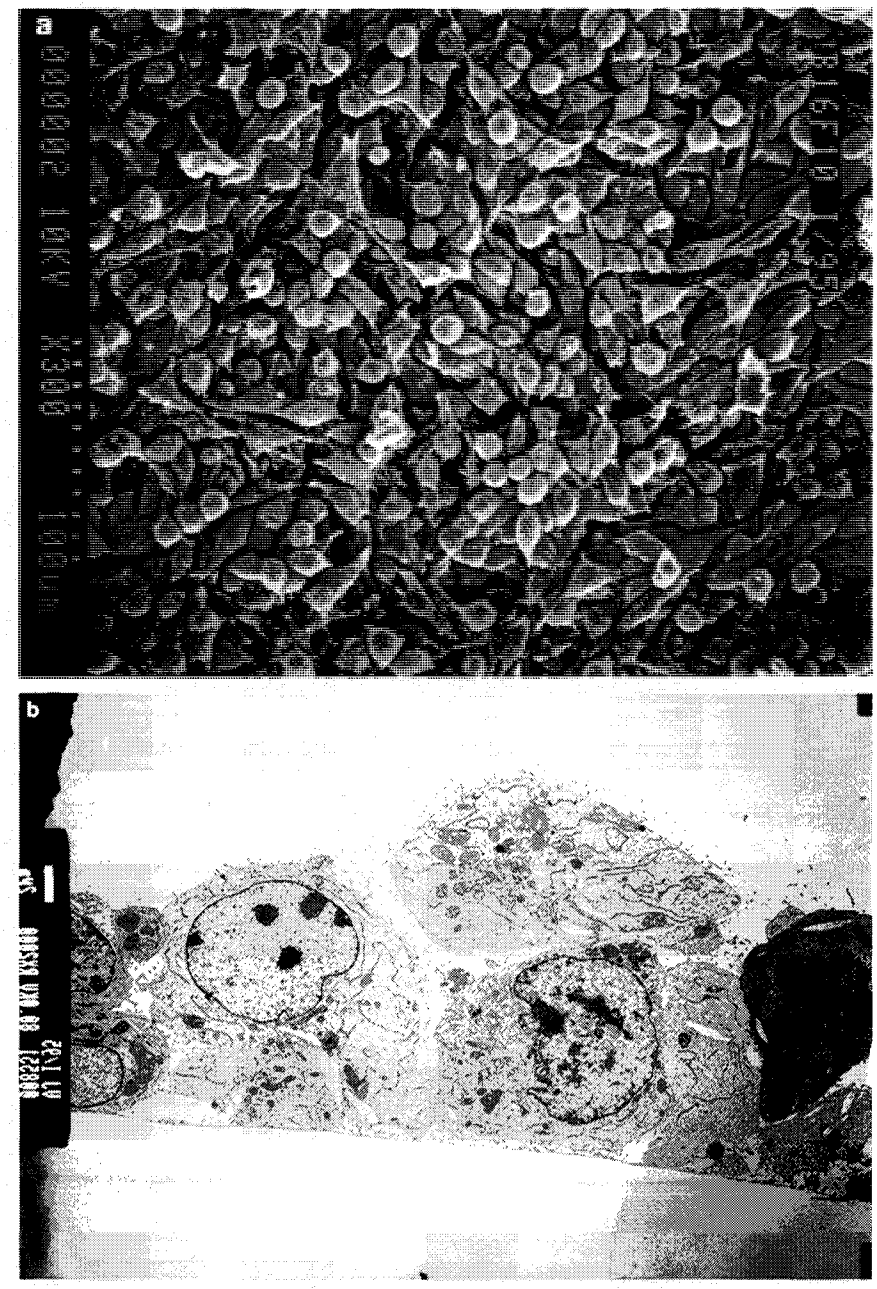

Fig. 2. Scanning (a) and transmission (b) electron micrographs of B16F10 cells grown on Matrigel® coated Transwell® inserts. In the images, the cell density is 3×10^6 cells/well. The dotted line in (a) is 100 μm; the white bar in (b) is 2 μm.

ing at approximately 2×10^5 antibody molecules per cell. In order to correct for non-specific binding in the a-TfR data, the concentration of a-DNP antibody bound at each time point was subtracted from the measured value of a-TfR bound. The resulting curve differs little from the uncorrected a-TfR data, indicating that non-specific binding contributes minimally to the a-TfR values. It should be noted that, since the temperature of the experiment was 37°C, the binding curves reflect not only binding to cell surface receptors, but also any internalization processes as well.

Figure 4 shows the relationship between the number of molecules bound per cell and antibody concentration for a-TfR at both 4°C and at 37°C. At 4°C, internalization is minimal, and binding is primarily to cell surface receptors. As shown by the 4°C data, the binding of a-TfR to the cell surface receptor is saturable in the concentration range 0 to 50 nM. Scatchard analysis of the data at 4°C gives an equilibrium affinity constant (K_a) of 6.3 (± 1.0) $\times 10^8$ M^{-1} and a receptor density of 1.1 (± 0.3) $\times 10^5$ per cell. The K_a value and receptor density are comparable to those reported by Ciechanover et al. (23) for the binding of transferrin to a human hepatoma cell line (HepG2) (2.3×10^8 M^{-1} and 6×10^4 receptors/cell) and by Sung et al. (24) for the binding of an anti-transferrin receptor immunotoxin to human rhabdo-

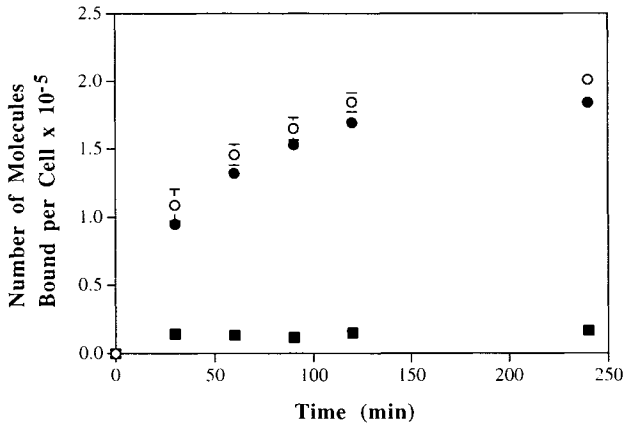

Fig. 3. Kinetics of binding of specific (a-TfR, ○) and non-specific (a-DNP, ■) antibodies to B16F10 cells. The curve labeled (●) is the difference between the a-TfR and a-DNP data, and represents the correction of a-TfR data for non-specific binding. n = 3.

myosarcoma cells (TE617) (2×10^9 M^{-1} and 4×10^4 receptors/cell).

Figure 4 also shows binding data at 37°C, which reflect both cell surface and intracellular binding. The more than twofold increase in the number of a-TfR antibodies associated with the cells at 37°C versus 4°C can be attributed to internalization. In addition, the apparent affinity constant at 37°C is 1.4 (±0.1) $\times 10^8$ M^{-1}, roughly one fourth of the value at 4°C. The shapes of the binding curves and the K_a values indicate that binding to cell surface anti-transferrin receptors (4°C) is a low capacity, high affinity process when compared to the high capacity, low affinity binding observed when internalization occurs (37°C). Internalization of anti-transferrin receptor antibodies is usually rapid (19), and is expected to account for a significant fraction of the total cell associated ligand in the two hour incubation period required to achieve steady-state binding. A limited number of similar binding experiments were conducted in Transwell® diffusion cells prepared as for the transport studies; the values for K_a (5.8×10^8 M^{-1}) and receptor density (2.5×10^5 per cell) at 37°C were of the same order of magnitude as those reported above for twelve-well plates.

Figure 5 shows the results of diffusive transport experiments conducted with the a-TfR and a-DNP antibodies at initial donor compartment concentrations of 10 nM (Fig. 5a) and 50 nM (Fig. 5b) and a temperature of 37°C. The relationship between receiver compartment concentration and time was approximately linear for both antibodies at both concentrations, suggesting steady-state conditions. The apparent permeabilities at 10 nM, calculated from the slopes of the linear portions of the curves ($t \geq 90$ min) according to equation 1, were 0.95×10^{-6} and 0.57×10^{-6} cm/s for the a-DNP and a-TfR antibodies, respectively. The difference in these slopes is significant at 95% confidence. This indicates that, under these conditions, the rate of diffusive transport of the binding a-TfR antibody is approximately half that of its isotype matched control. Similar results were obtained at a 50 nM donor concentration (Fig. 5b, Table I).

Additional features of Figures 5a and 5b should be noted. First, note that lag times are absent. In transport experiments of this type, a lag time is a period early in the study during which very little solute appears in the receiver compartment (25). The lag time reflects the time required to establish steady-state concentration profiles in the system, and may incorporate the time required for equilibration of rate processes acting *in series* with diffusional permeation. The absence of a lag time in these studies suggests that steady-state concentration profiles are established quickly, and that any rate processes that act in series with diffusional permeation equilibrate rapidly. Furthermore, the persistence of the differences in slope for the a-TfR and a-DNP antibodies throughout the experiment suggests that the rate process(es) responsible for altering the a-TfR permeabilities act *in parallel* with those that determine a-DNP permeability. Finally, note that the curve for the a-TfR antibody at 10 nM (Fig. 5a) is slightly nonlinear, and that the a-TfR and a-DNP curves are actually coincident for the first sixty minutes of the study. This feature is absent from the data at 50 nM (Fig. 5b), in which the a-TfR and a-DNP curves diverge at all times. This suggests that the parallel rate process (or processes) that alters permeability is established almost immediately at 50 nM, but requires approximately one hour to be fully evident at the lower concentration. Additional experiments were performed to probe the nature of these parallel processes; the results are presented below in the discussion of Table I.

Several technical issues related to these diffusion studies should also be noted. First, for the data in Figure 5a, the donor compartment concentration was greater than 9.2 nM for both antibodies at all times, indicating that the assumption of constant donor concentration is valid. Smaller donor compartment concentration changes (<2%) were observed at 50 nM. Mass balance calculations, in which the amounts of intact antibody (>10 kD) in the donor and receiver compartments and in the cell layer are summed, account for 90 to 110% of the initial antibody mass. In addition, both concentrations and the resulting permeability values have been corrected for low molecular weight fluorescence, and so reflect only the transport of material with molecular weight greater than 10 kD. The contributions of low molecular weight compounds to the total receiver compartment fluorescence at 240 minutes were 32% for the a-TfR antibody and 16% for

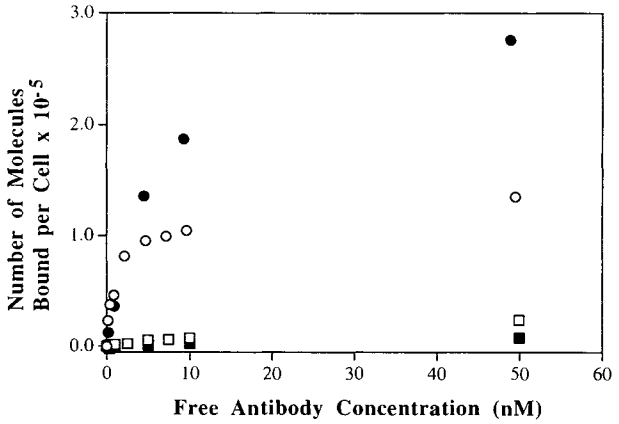

Fig. 4. Relationship between bound and free antibody concentrations for the binding of a-TfR antibody to B16F10 cells at 37°C (●) and at 4°C (○); data for a-DNP antibody at 37°C (■) and 4°C (□) are shown for comparison. n = 3.

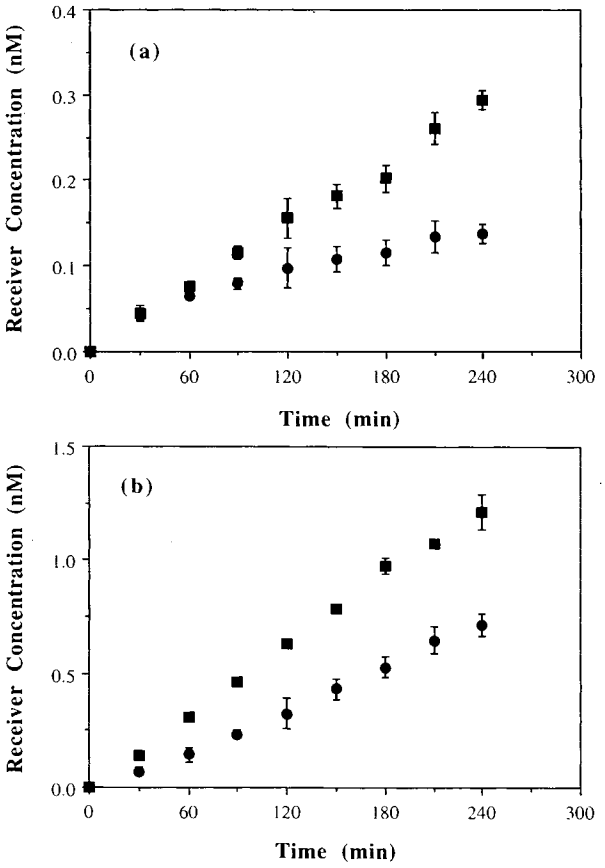

Fig. 5. Diffusion of specific (a-TfR, ●) and non-specific (a-DNP, ■) antibodies through B16F10 cell layers a donor concentrations of 10 nM (a) and 50 nM (b) and 37°C. n = 4 (a) and 3 (b).

the a-DNP antibody for the data in Figure 5a. In experiments at 50 nM donor concentrations (Fig. 5b) or at 4°C, the value was less than 10% of the total. This suggests that, while low molecular weight degradation products or free FITC are produced, they are not responsible for the majority of the transported material detected. Note that the measurement of low molecular weight fluorescence is not a direct measure of antibody degradation, since more than four FITC labels are bound to each molecule of antibody (see Analytical Methods) and antibody fragments may have differing molar absorptivity.

Table I summarizes the results of transport experiments conducted under a variety of experimental conditions. Lines 1 and 2 of the table show the measured permeabilities of the two antibodies at a 10 nM donor concentration both with (Line 2) and without (Line 1) cells present. Permeabilities in the absence of cells are approximately four times greater than those measured with cells. This difference indicates that the cells provide a significant diffusional barrier to antibody transport, comprising roughly 70 to 90% of the total resistance. Recall that the cell-free filter (Line 1) contains a cell-digested Matrigel precoating. The permeabilities in lines 2 through 8 have not been corrected for this background resistance, and thus are a reporting of observed values, corrected only for low molecular weight fluorescence.

Line 3 shows the measured permeabilities in a "blocking" experiment, in which the cells were pre-incubated with a ten-fold excess (100 nM) of an R-PE labelled ("cold") a-TfR antibody. In this case, the permeabilities of a-TfR and a-DNP antibodies were nearly equal. Excess cold a-TfR is expected to compete with labelled a-TfR for the transferrin receptor binding sites, greatly reducing the binding of the FITC-labeled antibody. The nearly identical permeability values for a-TfR and a-DNP in this experiment suggest that the difference observed in Line 2 is due to binding.

In order to distinguish between binding and internalization effects in the transport studies, experiments were performed at 4°C (Line 5) and in the presence of metabolic inhibitors (Line 4). At 4°C, internalization is expected to be minimal, with relatively little effect on equilibrium binding to surface receptors. However, the aqueous diffusivity and therefore the observed permeability are expected to decrease at a lower temperature, mainly due to the increased viscosity of the medium (5). In order to separate the effects of altered diffusivity and internalization, two approaches were taken. The first was the use of metabolic inhibitors that impair the internalization process while allowing experimentation at 37°C. In the second approach, a-DNP permeability was also measured at 4°C, to control for temperature effects on diffusivity. The data in Lines 4 and 5 show that there is little difference in a-TfR and a-DNP permeabilities at 4°C or in the presence of these inhibitors. This suggests that internalization contributes significantly to the difference in permeability reported in Line 2, and that this difference cannot be explained by binding to cell surface receptors alone. Note that the standard deviations in permeabilities in the presence of metabolic inhibitors (Line 4) are greater than others in the table. Light microscopy revealed that cell morphology, viability and adherence tended to be adversely affected by these inhibitors; these effects may contribute to the large standard deviations.

Line 6 shows the permeabilities at an initial donor compartment concentration of 50 nM. Recall that based on data at 4°C (Figure 4), binding of the a-TfR antibody to cell surface receptors saturates at approximately 10 nM. A 50 nM donor concentration is thus in excess of that required for equilibrium saturation of receptor binding. The results of Line 6 indicate that slower permeation of the a-TfR antibody is observed at 50 nM, and that the ratio of permeabilities is similar to that observed at 10 nM (Line 2; see also Fig. 5b). This result is consistent with the proposed roles of internalization and intracellular trafficking in determining a-TfR permeabilities in this system. If binding to cell surface receptors was the sole determinant of the difference in a-TfR and a-DNP permeabilities, concentrations sufficient to saturate cell surface receptors would be expected to result in equal a-TfR and a-DNP permeability values.

Line 7 shows the permeabilities at a 50 nM donor concentration and 4°C. This experiment duplicates that reported in Line 5, but at a higher donor concentration. Interestingly, a-TfR and a-DNP permeabilities differ at 50 nM and 4°C (Line 7), while they did not at 10 nM and 4°C (Line 5). At 4°C, internalization is prevented and cell surface receptors are saturated at both 10 and 50 nM (see Figure 4). Thus, the expected result for Line 7 is that a-TfR and a-DNP permeabilities are equal. That this is not observed cannot be fully explained, but may be due to a concentration dependence of

Table I. Permeabilities of Specific (a-TfR) and Non-specific (a-DNP) Antibodies in B16F10 Cell Layers Under Various Experimental Conditions

Line #	Experimental Conditions: Donor concentration, nM	Temperature, °C	Cell density, #/well × 10^6	Comments	Permeability, cm/s × 10^6 ± (SD)[a]: a-TfR	a-DNP	Permeability Ratio[b]: P(a-TfR)/P(a-DNP)
1	10	37	0	Filter only	4.8 (0.8)	4.6 (0.3)	1.04
2	10	37	3.0	Filter + cells	0.41 (0.03)	0.92 (0.03)	0.44
3	10	37	3.0	Ten-fold excess unlabelled a-TfR added (100 nM)	0.98 (0.04)	1.05 (0.04)	0.93
4	10	37	3.0	NaN_3 (25 mM) and 2-DG[c] (50 mM) added	1.2 (0.3)	1.0 (0.2)	1.20
5	10	4	3.0	Cold	0.62 (0.08)	0.69 (0.04)	0.90
6	50	37	3.0	Increased donor concentration	0.54 (0.04)	1.04 (0.04)	0.52
7	50	4	3.0	Increased donor concentration; cold	0.73 (0.05)	0.97 (0.02)	0.75
8	10	37	1.4	Reduced cell density	1.9 (0.2)	1.80 (0.08)	1.06
9	10	37	0.7	Reduced cell density	3.8 (0.1)	3.9 (0.1)	0.97

[a] Standard deviation of the mean, n = 3.
[b] Ratio of permeabilities (P) of a-TfR and a-DNP antibodies, calculated from values in the two previous columns.
[c] 2-DG = 2-deoxyglucose.

the a-DNP permeabilities, since a-DNP permeabilities are nearly 40% greater in Line 7 than in Line 5.

Lines 8 and 9 show the permeabilities at a 10 nM concentration and reduced cell densities. At 1.4 × 10^6 cells/well (Line 8), the cell layer is confluent; at 0.7 × 10^6 cells/well (Line 9), the layer is subconfluent. Under these conditions of reduced cell density, the a-TfR and a-DNP permeabilities are equal. This result should be contrasted with that reported in Line 2, where at high cell density differences in permeability were observed. The result suggests that the tissue penetration of a binding antibody will not be affected if cell and/or receptor density is insufficient. At the lowest cell density (Line 9), the measured permeabilities were not significantly different from those of the filter alone (Line 1), suggesting that the cell layer provides a negligible contribution to the total resistance to transport. At confluence (Line 8), the observed permeabilities are significantly different from the filter control, but the cell layer provided only 60% of the total resistance.

DISCUSSION

A cell culture model has been developed to investigate mechanistic aspects of the mass transport of antibodies in solid tumors. The model consists of a murine melanoma cell line, B16F10, grown on Matrigel® coated Transwell® filters, and is intended to represent a layer of cells in a tumor tissue. In general, tumors are composed of cells, extracellular matrix (stroma) and blood vessels, with the relative amount of each dependent on the type of tumor. The model proposed here primarily addresses the contributions of the cells to transport, since blood vessels are absent and extracellular matrix components are not present to an appreciable extent.

The approach presented here should be compared to previously reported in vitro models for studying mass transport in tumors. In 1974, Swabb et al. studied both diffusion and convection of various compounds through slices of tumor tissue (13), using a horizontally mounted diffusion cell. More recently, cultured spheroids of cells grown in suspension culture have been used by many groups to study diffusion (14). The spheroids are typically 50 to 100 cells in diameter, and may contain a necrotic core similar to that found in tumors in vivo. The agent of interest is added to the growth medium, and its depth of penetration over time is measured. Tumor penetration has also been studied in implanted "rabbit ear chambers" (15). In this method, a vascularized model tumor is formed by growing a malignant cell line in an implanted disc-shaped culture chamber, so that the penetration of labelled model compounds can be studied. Finally, Shockley and Yarmush have reported a novel in vitro system using hollow fibers (16). Malignant cells are cultured in the lumen of microporous hollow fibers. The agent of interest is added to the medium surrounding the fibers; the depth of penetration of the agent is determined by examining cross-sections of this "tumor cell cord."

The cultured cell layer approach presented here offers several useful features not found in the previously reported model systems. First, it allows for direct and convenient determination of diffusive permeabilities from concentrations in solution. In the spheroid, tumor cell cord and rabbit ear chamber models, permeabilities must be determined from concentration profiles measured in the model tissue.

Second, the present system allows for investigator control of the composition of the cell layer, particularly of cell density. In many of the previously reported systems, the cell layer may be poorly defined (as in the tissue slice model) or the cell density may be largely beyond the control of the investigator (as in the rabbit ear chamber). Finally, the system can be adapted to the study of convective (pressure gradient driven) transport. With the exception of the tumor slice model, the previously reported in vitro models do not allow for the controlled application of pressure gradients, either due to their geometry, as in the spheroid and tumor cell cord models, or due to homeostatic control by the animal as in the rabbit ear chamber.

The diffusive permeabilities determined here should be compared to values determined using these previously reported systems. Most published work reports effective diffusion coefficients (D_{eff}) rather than permeabilities. D_{eff} values can be estimated from experimentally determined permeabilities by multiplying by the cell layer thickness. Using a cell layer thickness of approximately 15 μm (see Figure 2) and the permeability values reported in Table I, the D_{eff} values determined here are approximately 0.5 to 1.0 $\times$ 10^{-9} cm^2/sec. In studies of antibody permeation in human melanoma cell spheroids, Kwok et al. found a D_{eff} value of 4.5 $\times$ 10^{-9} cm^2/sec for a binding IgG_{2a} antibody (26). In the tumor cell cord model, Shockley and Yarmush determined an effective diffusion coefficient for a nonbinding monoclonal antibody in human melanoma cells of approximately 1 $\times$ 10^{-9} cm^2/sec (16). Using the rabbit ear chamber, Clauss and Jain measured D_{eff} for nonspecific polyclonal IgG in VX2 carcinoma tissue, and obtained values of 1.4 $\times$ 10^{-8} and 6.3 $\times$ 10^{-9} cm^2/sec (15). Our values compare favorably with these previously reported results. In a way, this consistency is somewhat surprising, since the cell lines and target antigens (if any) vary among these systems. In all cases, however, the tissue is a dense cellular region with little extracellular matrix; this similarity may be important in determining the measured diffusion coefficients. It should be noted that, due to antibody size and the limited junctional contacts between the cells, significant paracellular diffusion of antibody is expected in all these systems.

Cell-culture based models such as the one presented here are perhaps most useful for addressing transport mechanisms. The results presented above demonstrate that, under certain conditions, diffusion of the binding antibody (a-TfR) is significantly slower than that of the indifferent control (a-DNP). Blocking experiments (Table I, Line 3) suggest that this difference is due to antibody binding. These results are consistent with the "binding site barrier" hypothesis (9,10), which states that the penetration of binding antibodies in tumors should be slowed by their binding to tumor antigens. However, additional experiments at reduced temperature (Table I, Lines 5 and 7) and in the presence of metabolic inhibitors (Table I, Line 4) suggest that the internalization and recycling of the antibody/antigen complex are important in slowing penetration of the a-TfR antibody in this system. In addition, the shapes of the permeation curves (Figure 5) indicate that permeation is slowed by process(es) acting in parallel with extracellular diffusion. On the basis of these results, we hypothesize that internalization and recycling of the antibody act in parallel with extracellular diffusion to slow the transport of the a-TfR antibody in this system. The binding, internalization and recycling of the a-TfR antibody can thus be conceptualized as a kind of "detour" in its permeation through the cell layer, lengthening the total time required for permeation relative to that of the nonbinding control. This detour is essentially unavailable to the a-DNP antibody, which is not bound, internalized or recycled to an appreciable extent.

In a detailed study of the kinetics of transferrin receptor cycling, Ciechanover et al. estimated the times required for transferrin binding, internalization and return of the receptor to the cell surface in HepG2 cells; the values were 4.3, 5.0 and 7.2 minutes, respectively (23). The processes of internalization and receptor return to the cell surface thus contribute significantly to the total time required for transferrin receptor cycling in HepG2, which Ciechanover et al. estimate as approximately 17 minutes. In the present studies, inhibition of internalization was found to influence the rate of diffusive transport; this result is consistent with the importance of internalization and receptor return in transferrin receptor cycling.

To the extent that this cell culture system serves as a model for cell-dense regions of a solid tumor, the results have implications for the use of immunoconjugates in chemotherapy. The rate of permeation of the a-TfR antibody was approximately half that of the control at 10 and 50 nM donor concentrations and 37°C (see Table I), suggesting that binding does slow antibody transport. As noted above, this result is in keeping with the "binding site barrier" hypothesis. However, differences in transport of a-TfR and control antibodies were observed only at high cell densities (see Table I). Thus, the "binding site barrier" may be important clinically only in tumor regions in which cell density is relatively high. In addition, the studies at reduced temperature and with metabolic inhibitors (see Table I) demonstrate that antibody internalization influences the observed permeation rate in this system. This suggests that events occurring subsequent to antibody binding, such as internalization and the intracellular trafficking of the antibody/antigen complex, may influence the overall tumor permeation rate. Additional studies are required to relate binding and internalization rates to permeation in a more quantitative way, and to define the molecular weight and binding ability of the permeant molecules which may have been altered during transport. Finally, it should be noted that the studies presented here address only transport occurring by diffusion. As discussed in the introduction, convection is also thought to play a role in immunoconjugate penetration, particularly in larger tumors. The results presented here are thus most directly applicable to smaller tumors or to tumor microregions, in which convective transport is less important.

ACKNOWLEDGMENTS

The authors wish to thank Dr. Paul Kitos of the University of Kansas Division of Biology for his assistance with the cell culture methods, Dr. Bruce Cutler of the University of Kansas Electron Microscopy lab for his assistance with electron microscopy, and Dr. Vincent Hearing of the National Cancer Institute for his helpful comments. The authors gratefully acknowledge financial support from the Whitaker Foundation.

REFERENCES

1. D. M. Goldenberg, Monoclonal antibodies in cancer detection and therapy, *Am. J. Med.*, 94:297–312 (1993).
2. G. A. Peitersz and I. F. C. McKenzie, Antibody conjugates for the treatment of cancer, *Immunol. Rev.*, 129:57–80 (1992).
3. W. C. Shen, S. Persiani, B. Ballou and T. R. Hakala, Antibodies as drug carriers for solid tumors: evaluation of drug-anti-SSEA-1 conjugates in the treatment of teratocarcinoma. In *Targeted Therapeutic Systems*, P. Tyle and B. P. Ram (Eds.), Marcel Dekker, Inc., New York, 1990, pp. 289–304.
4. R. Pirker, Immunotoxins against solid tumors. *J. Cancer Res. Clinical Oncol.*, 114:385–393 (1988).
5. R. K. Jain, Transport of molecules in the tumor interstitium: a review, *Cancer Res.*, 47:3039–3051 (1987).
6. R. K. Jain, Transport of molecules across tumor vasculature, *Cancer Metastasis Rev.*, 6:559–593 (1987).
7. L. M. Cobb, Intratumour factors influencing the access of antibody to tumour cells, *Cancer Immunol. Immunother.*, 28:235–240 (1989).
8. R. K. Jain, Barriers to drug delivery in solid tumors, *Sci. Am.*, 271:58–65 (1994).
9. K. Fujimori, D. G. Covell, J. E. Fletcher and J. N. Weinstein, A modeling analysis of monoclonal antibody percolation through tumors: a binding-site barrier, *J. Nuclear Med.*, 31:1191–1198 (1990).
10. M. Juweid, R. Neumann, C. Paik, M. J. Perez-Bacete, J. Sato, W. van Osdol and J. N. Weinstein, Micropharmacology of monoclonal antibodies in solid tumors: direct experimental evidence for a binding site barrier, *Cancer Res.*, 52:5144–5153 (1992).
11. K. Lin, J. A. Nagy, H. Xu, T. R. Shockley, M. L. Yarmush and H. F. Dvorak, Compartmental distribution of tumor-specific monoclonal antibodies in human melanoma xenografts, *Cancer Res.*, 54:2269–2277 (1994).
12. C. Sung, R. L. Dedrick, W. A. Hall, P. A. Johnson and R. J. Youle, The spatial distribution of immunotoxins in solid tumors: assessment by quantitative autoradiography, *Cancer Res.*, 53:2092–2099 (1993).
13. E. A. Swabb, J. Wei and P. M. Gullino, Diffusion and convection in normal and neoplastic tissues. *Cancer Res.*, 34:2814–2822 (1974).
14. R. M. Sutherland, Cell and environment interactions in tumor microregions: the multicell spheroid model. *Science*, 240:177–184 (1988).
15. M. A. Clauss and R. K. Jain, Interstitial transport of rabbit and sheep antibodies in normal and neoplastic tissues. *Cancer Res.*, 50:3487–3492 (1990).
16. T. R. Shockley and M. L. Yarmush, Growth of tumor cells within microporous hollow fibers: as in vitro model system for studies of immunoprotein transport, *Biotechnol. Bioeng.*, 35:843–849 (1990).
17. L. T. Baxter and R. K. Jain, Transport of fluid and macromolecules in tumors. III. Role of binding and metabolism. *Microvascular Res.*, 41:5–23 (1991).
18. K. Fujimori, D. R. Fisher and J. N. Weinstein, Integrated microscopic-macroscopic pharmacology of monoclonal antibody radioconjugates: the radiation dose distribution. *Cancer Res.*, 51:4821–4827 (1991).
19. J. A. Hanover and R. B. Dickson, Transferrin: receptor-mediated endocytosis and iron delivery, in *Endocytosis*, I. Pastan and M. C. Willingham (Eds.), Plenum Press, 1985, pp. 131–161.
20. G. L. Nicolson, T. Inoue, C. S. Van Pelt and P. G. Cavanaugh, Differential expression of a Mr 90,000 cell surface transferrin receptor-related glycoprotein on murine B16 metastatic melanoma sublines selected for enhanced brain or ovary colonization, *Cancer Res.*, 50:515–520 (1990).
21. E. L. Cussler, *Diffusion: Mass Transfer in Fluid Systems*. Cambridge University Press, New York, 1984, pp. 21–32.
22. M. Brinkley, A brief survey of methods for preparing protein conjugates with dyes, haptens and cross-linking reagents. *Bioconjug. Chem.*, 3:2–13 (1992).
23. A. Ciechanover, A. L. Schwartz, A. Dautry-Varsat and H. F. Lodish, Kinetics of internalization of recycling of transferrin and the transferrin receptor in a human hepatoma cell line, *J. Biol. Chem.*, 258:9681–9689 (1983).
24. C. Sung, R. J. Youle, R. L. Dedrick, Pharmacokinetic analysis of immunotoxin uptake in solid tumors: role of plasma kinetics, capillary permeability and binding, *Cancer Res.*, 50:7382–7392 (1990).
25. Crank, J., *The Mathematics of Diffusion*, 2nd ed. Oxford University Press, New York, 1975, pp. 49–53.
26. C. S. Kwok, S. E. Cole and S. K. Liao, Uptake kinetics of monoclonal antibodies by human malignant melanoma spheroids, *Cancer Res.*, 48:1856–1863 (1988).